Brain Struct Funct (2011) 216:239–254
DOI 10.1007/s00429-011-0301-5

ORIGINAL ARTICLE

The receptor architecture of the pigeons' nidopallium caudolaterale: an avian analogue to the mammalian prefrontal cortex

Christina Herold · Nicola Palomero-Gallagher · Burkhard Hellmann · Sven Kröner · Carsten Theiss · Onur Güntürkün · Karl Zilles

Received: 26 October 2010 / Accepted: 12 January 2011 / Published online: 4 February 2011

Abstract The avian nidopallium caudolaterale is a multimodal area in the caudal telencephalon that is apparently not homologous to the mammalian prefrontal cortex but serves comparable functions. Here we analyzed binding-site densities of glutamatergic AMPA, NMDA and kainate receptors, GABAergic $GABA_A$, muscarinic M_1, M_2 and nicotinic (nACh) receptors, noradrenergic α_1 and α_2, serotonergic 5-HT_{1A} and dopaminergic D_1-like receptors using quantitative in vitro receptor autoradiography. We compared the receptor architecture of the pigeons' nidopallial structures, in particular the NCL, with cortical areas Fr2 and Cg1 in rats and prefrontal area BA10 in humans. Our results confirmed that the relative ratios of multiple receptor densities across different nidopallial structures (their "receptor fingerprints") were very similar in shape; however, the absolute binding densities (the "size" of the fingerprints) differed significantly. This finding enables a delineation of the avian NCL from surrounding structures and a further parcellation into a medial and a lateral part as revealed by differences in densities of nACh, M_2, kainate, and 5-HT_{1A} receptors. Comparisons of the NCL with the rat and human frontal structures showed differences in the receptor distribution, particularly of the glutamate receptors, but also revealed highly conserved features like the identical densities of $GABA_A$, M_2, nACh and D_1-like receptors. Assuming a convergent evolution of avian and mammalian prefrontal areas, our results support the hypothesis that specific neurochemical traits provide the molecular background for higher order processes such as executive functions. The differences in glutamate receptor distributions may reflect species-specific adaptations.

Keywords Receptor autoradiography · Prefrontal cortex · Nidopallium caudolaterale · Rat · Human · Fr2 · Cg1 · BA10 · Dopamine · Glutamate · GABA

Abbreviations

ACh	Acetylcholine
AMPA	α-Amino-3-hydroxy-5-methyl-4-isoxalone propionic acid
Cg1	Cingulate cortex 1
CDL	Dorsolateral corticoid area
EPSCs	Excitatory postsynaptic currents
FR2	Frontal area 2
GABA	γ-Aminobutyric acid
GLI	Gray level index
gluR1	Glutamate receptor subunit 1
HA	Hyperpallium apicale
HVC	Higher vocal center
IMM	Intermediate and medial mesopallium ventrale

C. Herold (✉) · K. Zilles
C. and O. Vogt-Institute of Brain Research, University of Düsseldorf, 40225 Düsseldorf, Germany
e-mail: christina.herold@uni-duesseldorf.de

N. Palomero-Gallagher · K. Zilles
Institute of Neuroscience and Medicine INM-2, Research Center Jülich, 52425 Jülich, Germany

B. Hellmann · O. Güntürkün
Department of Biopsychology, Institute of Cognitive Neuroscience, Faculty of Psychology, Ruhr-University Bochum, 44780 Bochum, Germany

C. Theiss
Institute of Anatomy and Molecular Embryology, Faculty of Medicine, Ruhr-University Bochum, 44780 Bochum, Germany

S. Kröner
School of Behavioral and Brain Sciences, The University of Texas at Dallas, Richardson, TX 75080, USA

MNH	Mediorostral nidopallium/hyperpallium
nACh	Nicotinic acetylcholine
NCC	Nidopallium caudocentrale
NCL	Nidopallium caudolaterale
NCLl	Nidopallium caudolaterale pars lateralis
NCLm	Nidopallium caudolaterale pars medialis
NCM	Nidopallium caudomediale
NFT	Nidopallium fronto-trigeminale
NIM	Nidopallium intermedium medialis
NMDA	*N*-methyl-D-aspartate
PFC	Prefrontal cortex

Introduction

The increasingly refined parcellation of the mammalian cerebral cortex with anatomical methods enables various analyses of its functional segregation (Uylings et al. 2000; Amunts et al. 2004; Eickhoff et al. 2006, Amunts et al. 2007; Naito et al. 2008; Palomero-Gallagher et al. 2009; Zilles and Amunts 2010). Similarly, in the last decades the avian forebrain has been subdivided by various means. These efforts have fostered a new understanding of the avian telencephalic organization and the assumed homologies between avian and mammalian brain components (Reiner et al. 2004). This new view, which is rooted in a series of seminal studies over the last 40 years (Karten 1969), assumes that mammalian and avian pallia are homologous in terms of shared pallial identity that derive from common ancestry (Jarvis et al. 2005). This assumption, however, does not imply that cortical or subcortical pallial areas have to be one-to-one homologous to pallial components in birds. Thus, pallial structures of birds and mammals might be similar in terms of anatomical, physiological and cognitive characteristics, but may still represent the result of convergent evolution.

The avian nidopallium caudolaterale (NCL) is such a case. Numerous studies show that the mammalian prefrontal cortex (PFC) and the avian NCL share several anatomical (Kröner and Güntürkün 1999), neurochemical (Bast et al. 2002; Karakuyu et al. 2007), electrophysiological (Diekamp et al. 2002a; Kalenscher et al. 2005; Rose and Colombo 2005), and functional (Güntürkün 1997; Diekamp et al. 2002b; Kalenscher et al. 2003; Lissek and Güntürkün 2005) characteristics; however, several genetic (Puelles et al. 2000) and topological arguments (Medina and Reiner 2000) make a homology between the PFC and the NCL unlikely. Therefore, the similarities of these two structures likely do not result from common ancestry but represent the outcome of an evolutionary convergence. Thus, a common selection pressure for an 'executive' behavioral repertoire possibly facilitates emergence of non-homologous forebrain areas of mammals and birds that share typical 'prefrontal' characteristics (Güntürkün 2005a; Kirsch et al. 2008).

The NCL displays a homogeneous cytoarchitecture and does not differ considerably from neighboring portions of the nidopallium either. The NCL was first defined by its dopaminergic innervation and high tyrosine hydroxylase density (Divac et al. 1985; Waldmann and Güntürkün 1993). To date, the outer borders and the internal structure of the NCL have been analyzed with immunocytochemical (Wynne and Güntürkün 1995; Bock et al. 1997; Schnabel et al. 1997; Durstewitz et al. 1998; Riters et al. 1999) and ultrastructural methods (Metzger et al. 2002) as well as in several tracing studies (Leutgeb et al. 1996; Metzger et al. 1998; Kröner and Güntürkün 1999). Receptor autoradiography is an additional powerful tool to define areal borders and to derive region-specific receptor-density combinations that define areas like 'fingerprints' (Zilles et al. 2002b). Therefore, the first aim of this study was to map the chemoarchitecture of the NCL. This approach is important to define the areal borders between the nidopallium caudocentrale (NCC) and the NCL, since different studies using tracing techniques or immunocytochemistry showed discrepant delineations (Wynne and Güntürkün 1995; Waldmann and Güntürkün 1993; Kröner and Güntürkün 1999; Atoji and Wild 2009). Although, the border to the laterally and supraventricular located dorsolateral corticoid area (CDL) and the NCL is easier to define, it was additionally included in the analysis here.

The second aim of this study was to investigate possible subdivisions within the NCL because numerous studies in mammals have implicated subdivisions of the PFC in the processing of different stimulus domains (Levy and Goldman-Rakic 1999). Similarly, there is also evidence for a parcellation of the NCL based on functional, neurochemical and hodological data (Leutgeb et al. 1996; Braun et al. 1999; Kröner and Güntürkün 1999; Riters et al. 1999; Diekamp et al. 2002b). Riters et al. (1999) proposed a dorsoventral distinction of the NCL based on the distribution of tyrosine hydroxylase, choline acetyltransferase and substance P labeled fibers and terminals. Accordingly, lesions of the dorsal NCL result in delay-specific working memory deficits (Diekamp et al. 2002b). The high density of tyrosine hydroxylase positive fibers in the dorsal NCL might be related to the important role of dopamine in working memory functions as shown in primates (Goldman-Rakic 1999) and birds (Karakuyu et al. 2007). Based on connectivity data, however, Kröner and Güntürkün (1999) assumed a frontocaudal distinction with the caudal portion being tightly embedded within the limbic system.

The third aim was to compare the receptor fingerprints of mammalian frontal and prefrontal areas with those of the avian NCL in order to examine whether a common

functional repertoire is reflected by a similar pattern of receptor architecture. For this purpose we studied the receptor fingerprints of the medial and the lateral portions of Brodmann's human prefrontal cortex area BA10 (BA10m and BA10l, respectively) and the rat frontal area 2 (Fr2) as well as the rat prefrontal cingulate area 1 (Cg1) (Brodmann 1909; Uylings et al. 2003). Owing to their connectivity patterns with other neocortical areas, the thalamus, the basal ganglia, and the amygdala, both Fr2 and Cg1 were structurally and functionally compared with the dorsolateral prefrontal cortex in primates (Uylings et al. 2003; Van de Werd et al. 2010). However, it has to be noted they there are still discrepancies in the delineations of rat prefrontal and motor cortical structures; furthermore, Fr2 is classified as the rodent's motor cortex (Van Eden et al. 1992; Zilles 1985).

Taken together, our receptor autoradiographic study was aimed to constitute an independent approach to these open questions.

Materials and methods

We examined a total of six pigeons (*Columba livia*) of unknown sex and eight male rats (*Long-Evans*). Animals were decapitated and the brains removed from the skull, frozen immediately in isopentane at −40°C and stored at −70°C. Serial coronal 10 µm sections were cut with a cryostat microtome (2800 Frigocut E, Reichert-Jung). Sections were thaw-mounted on gelatinized slides and freeze-dried.

Post-mortem human brain tissue was studied from 2 control subjects (age 72 male and age 77 female, post-mortem time 8 and 18 h) without a record of neurological or psychiatric disorders and was obtained from the body donor program of the Department of Anatomy, University of Düsseldorf, Germany. Causes of death were a heart attack and carcinoma. Serial coronal cryosections (20 µm) comprising the whole cross-section of unfixed brain blocks were prepared at −20°C using a large-scale cryostat microtome. Sections were thaw-mounted on gelatinized slides, freeze-dried and stained with a modified cell body staining for cytoarchitectonic analysis (Merker 1983; Palomero-Gallagher et al. 2008) or processed for receptor autoradiography.

Receptor autoradiography

Details of the autoradiographic labeling procedure have been published elsewhere (Zilles et al. 2002b; Palomero-Gallagher et al. 2009). Binding protocols are summarized in Table 1. Three steps were performed in the following sequence: (1) A preincubation step removed endogenous ligand from the tissue. (2) During the main incubation step, binding sites were labeled with triated ligand (total binding). Coincubation of the triated ligand and a 1,000 to 10,000-fold excess of an appropriate non-labeled ligand (displacer) determined non-specific and thus non-displaceable binding. Specific binding is the difference between total and non-specific binding. (3) A final rinsing step eliminated unbound radioactive ligand from the sections.

The following binding sites were labeled according to standardized protocols: α-amino-3-hydroxy-5-methyl-4-isoxalone propionic acid (AMPA) with [^{3}H] AMPA, kainate with [^{3}H]kainate, *N*-methyl-D-aspartate (NMDA) with [^{3}H]MK-801, γ-aminobutyric acid A ($GABA_A$) receptor with [^{3}H]muscimol, muscarinic cholinergic M_1 receptor with [^{3}H]pirenzepine, muscarinic cholinergic M_2 receptor with [^{3}H]oxotremorine-M, nicotinic cholinergic (nACh) receptor with [^{3}H]cytosine (pigeon) or [^{3}H]epibatidine (rat and human), noradrenergic α_1 adrenoreceptor with [^{3}H]prazosin, noradrenergic α_2 adrenoreceptor with [^{3}H] RX-821002, serotonergic 5-HT_{1A} receptor with [^{3}H]8-OH-DPAT, and dopaminergic D_1-like receptors with [^{3}H]SCH 23390. Sections were air-dried overnight and subsequently coexposed for 4–5 weeks against a tritium-sensitive film (Hyperfilm, Amersham, Braunschweig, Germany) with plastic [^{3}H]-standards (Microscales, Amersham) of known concentrations of radioactivity.

Image analysis

The resulting autoradiographs were subsequently processed using densitometry with a video-based image analyzing technique (Zilles et al. 2002b; Schleicher et al. 2005). Autoradiographs were digitized by means of a KS-400 image analyzing system (Kontron, Germany) connected to a CCD camera (Sony, Tokyo) equipped with a S-Ortho-planar 60-mm macro lens (Zeiss, Germany). The images were stored as binary files with a resolution of 512 × 512 pixels and 8-bit gray value. The gray value images of the coexposed microscales were used to compute a calibration curve by non-linear, least-squares fitting, which defined the relationship between gray values in the autoradiographs and concentrations of radioactivity. This enabled the pixel-wise conversion of the gray values of an autoradiograph into the corresponding concentrations of radioactivity. These concentrations of binding sites occupied by the ligand under incubation conditions are transformed into fmol binding site/mg protein at saturation conditions by means of the equation: $(K_D + L)/A_S \times L$, where K_D is the equilibrium dissociation constant of ligand-binding kinetics, L is the incubation concentration of ligand, and A_S the specific activity of the ligand. The mean of the gray values contained in a specific region over a series of 4–5 sections

Table 1 Incubation conditions for receptor autoradiography

Receptor	[^{3}H] ligand (incubation concentration)	Displacer (incubation concentration)	Incubation buffer	Preincubation step	Main incubation step	Rinsing step
AMPA	[^{3}H]AMPA (10 nM)	Quisqualate (10 μM)	50 mM Tris–acetate (pH 7.2)	3 × 10 min at 4°C in incubation buffer	45 min at 4°C in incubation buffer + 100 mM KSCN	4 × 4 s at 4°C in incubation buffer + 2 × 2 s at 4°C in acetone/glutaraldehyde
Kainate	[^{3}H]kainate (8 nM)	Kainate (100 μM)	50 mM Tris–citrate (pH 7.1)	3 × 10 min at 4°C in incubation buffer	45 min at 4°C in incubation buffer + 10 mM Ca-acetate	4 × 4 s at 4°C in incubation buffer + 2 × 2 s at 4°C in acetone/glutaraldehyde
NMDA	[^{3}H]MK-801 (5 nM)	MK-801 (100 μM)	50 mM Tris–HCl (pH 7.2)	15 min at 25°C in incubation buffer	60 min at 25°C in incubation buffer + 30 μM glycine + 50 μM spermidine	2 × 5 min at 4°C in incubation buffer
Muscarinergic cholinergic M_1	[^{3}H]pirenzipine (1nM)	Pirenzipine (10 μM)	Modified Krebs–Ringer buffer (pH 7.4)	20 min at 25°C in incubation buffer	60 min at 25°C in incubation buffer	2 × 5 min at 4°C in incubation buffer
Muscarinergic cholinergic M_2	[^{3}H]oxotremonine-M (0.8 nM)	Carbachol (1 μM)	20 mM Hepes–Tris (pH 7.5) + 10 mM $MgCl_2$	20 min at 25°C in incubation buffer	60 min at 25°C in incubation buffer	2 × 2 min at 4°C in incubation buffer
Nicotinic cholinergic	[^{3}H]cytisine [1 nM]	Nicotine (10 μM)	50 mM Tris–HCl (pH7.4) + 120 mM NaCl + 5 mM KCl + 1 mM $MgCl_2$ + 2.5 mM $CaCl_2$	15 min at 22°C in incubation buffer	90 min at 4°C in incubation buffer	2 × 2 min at 4°C in incubation buffer
	[^{3}H]epibatidine [0.5 nM]	Nicotine (10 μM)	15 mM Hepes–Tris (pH 7.5) + 10 mM NaCl + 5.4 mM KCl + 0.8 mM $MgCl_2$ + 1.8 mM $CaCl_2$	20 min at 22°C in incubation buffer	90 min at 4°C in incubation buffer	1 × 5 min at 4°C in incubation buffer 2 × up & down in distilled H_2O
α_1 Adrenoreceptor	[^{3}H]prazosin (0.2 nM)	Phentolamine (10 μM)	50 mM Tris–HCl (pH 7.4)	30 min at 37°C in incubation buffer	45 min at 30°C in incubation buffer	2 × 5 min at 4°C in incubation buffer
α_2 Adrenoreceptor	[^{3}H]UK-14304 (1.4 nM)	Noradrenalin (100 μM)	50 mM Tris–HCl (pH 7.7) + 100 μM $MnCl_2$	15 min at 22°C in incubation buffer	90 min at 22°C in incubation buffer	5 min at 4°C in incubation buffer
$GABA_A$	[^{3}H]muscimol (6 nM:pigeon and 3 nM:human)	GABA (10 μM)	50 mM Tris–citrate (pH 7.0)	3 × 5 min at 4°C in incubation buffer	40 min at 4°C in incubation buffer	3 × 3 s at 4°C in incubation buffer
Serotoninergic 5-HT_{1A}	[^{3}H]8-OH-DPAT (1 nM)	Serotonin (10 μM)	170 mM Tris–HCl (pH 7.6) + 4 mM $CaCl_2$ + 0.01% ascorbic acid	30 min at 22°C in incubation buffer	60 min at 22°C in incubation buffer	1 × 5 min at 4°C in incubation buffer
Dopaminergic D_1-like	[^{3}H]SCH-23390 (0.5 nM)	SKF 83566 (1 μM)	50 mM Tris–HCl (pH 7.4) + 120 mM NaCl + 5 mM KCl + 2 mM $CaCl_2$ + 1 mM $MgCl_2$ + 1 μM mianserin	20 min at 22° C in incubation buffer	90 min at 22° C in incubation buffer	2 × 10 min at 4° C in incubation buffer

from one animal is thus transformed into a receptor concentration (fmol/mg protein).

Anatomical identification

The borders of the NCL were identified based on previous neurochemical (Waldmann and Güntürkün 1993) and tract-tracing studies (Kröner and Güntürkün 1998). The borders of the NCL and surrounding structures as defined in the atlas of Karten and Hodos (1967) were traced on prints of the digitized autoradiographs. The borders of rat Fr2 and Cg1 were anatomically identified based on a rat cortex atlas (Zilles 1985). We decided to analyze these two regions because they are assumed to be a part of the rat frontal and prefrontal cortex (Uylings et al. 2003). The borders of human BA10 were identified based on criteria defined by Brodmann (Brodmann 1909). BA10m and BA10l were additionally defined and traced onto digitized autoradiographs ($n = 3$ hemispheres). The mean of the gray values contained in a specific region over a series of 4–5 sections from one hemisphere is thus transformed into a receptor concentration per unit protein (fmol/mg protein).

Statistical analysis

To investigate the chemoarchitectural differences between the NCL and the surrounding structures, the binding site concentrations of the NCL were compared with those of the nidopallium caudomediale (NCM, located medial to NCL) and the dorsolateral corticoid area (CDL, located dorsolaterally to NCL, above the ventricle). First, a Friedman ANOVA was conducted. If significant, pair wise comparisons were run with the Wilcoxon rank test. Binding site concentrations of the NCM were measured medial to Field L. Differences between nidopallium caudolaterale pars medialis (NCLm) and nidopallium caudolaterale pars lateralis (NCLl) were further analyzed with Wilcoxon rank tests.

Results

Receptor-binding site densities in avian pallial structures

The most caudal portion of the avian nidopallium displays a rather homogeneous cytoarchitecture. The only subventricular cytoarchitectural feature that is clearly different from the otherwise homogeneous pattern is Field L in the most medial part. Within Field L, especially, the granular layer L2 is readily visible. Ventrolaterally, the lamina arcopallialis dorsalis defines the borderline between the nidopallium and the arcopallial and the amygdalar substructures. Dorsally, the caudal cap of the lateral ventricle separates the nidopallium from the CDL and the hippocampal and parahippocampal structures. The distribution of different ligand-binding sites shows that the cytoarchitectonically seemingly homogeneous caudal nidopallium is in fact comprised of several substructures. Further, the examined receptor types not only enabled a clear delineation of the NCL from the adjoining areas, but also revealed the existence of two hitherto unknown subentities. Stereotaxic coordinates, A 5.50 and A 6.75, were chosen as exemplary levels for which all receptor types were shown in Fig. 1a and b. Different binding-site densities within the borders of the NCL could be followed up to the most caudal aspect of the subventricular forebrain where it constituted the most caudal tip of the nidopallium. Frontally, the NCL was visible up to A 7.50 (anterior–posterior coordinates according to the pigeon brain atlas of Karten and Hodos 1967). Further, binding-site densities of the different receptor ligands are presented relative to each other in a 2-dimensional coordinate plot to construct a receptor fingerprint for a given brain area (Fig. 2). This allows us to compare the shape and the absolute size of this receptor fingerprint across brain areas and between species.

As illustrated in the autoradiographs and in the fingerprints, glutamatergic AMPA and NMDA receptors show the highest densities of all measured receptors, and were followed by $GABA_A$ receptor densities. Conversely, lowest values were found for nACh, α_1 and D_1-like receptor densities (Figs. 1a/b, 2a).

The mean density of AMPA receptors for the whole NCL was 2,252 ± 269 fmol/mg protein. A comparison of binding densities between NCL, NCC and CDL using a Friedman ANOVA showed no significant overall effects [Chi Square ($N = 6$, df = 2) = 1, n.s.].

Overall densities for kainate receptor-binding sites were 660 ± 81 fmol/mg (Fig. 1a/b). Because kainate receptor-binding sites were approximately fivefold lower than those of AMPA receptors, and sixfold lower than those of NMDA receptors, this resulted in a considerable indentation in the fingerprint (Fig. 2a). Binding of [^{3}H]kainate was highest in the most lateral portion of the NCL (Figs. 1a/b, 3). We labeled this area nidopallium caudolaterale pars lateralis (NCLl) to differentiate it from the medial portion of the NCL (NCLm). The Friedman ANOVA showed a significant overall effect [Chi Square ($N = 6$, df = 2) = 10.33, $p < 0.01$]. Binding was higher both in NCL and NCC than in CDL (all $N = 6$, $T = 0$, $p < 0.05$). Additionally, a significant higher concentration of kainate receptors in the lateral than in the medial aspect of the NCL was detected ($N = 6$, $T = 1$, $p < 0.05$; Fig. 3).

Binding of [^{3}H]MK-801 was very high throughout the entire caudal nidopallium (Fig. 1a/b), indicating a high

density of NMDA receptors. Binding density reached 2,525 ± 143 fmol/mg protein (Figs. 1a, 2a) in NCL. Like for the AMPA receptors this results in a prominent peak in the fingerprints (c.f Fig. 2a). The Friedman ANOVA comparing NCL, NCC and CDL showed a significant overall effect [Chi Square ($N = 6$, df $= 2$) $= 8.33$, $p < 0.05$]. A subsequent Wilcoxon test revealed significantly higher values for NCL and NCM over CDL (all $N = 6$, $T \leq 1$, $p < 0.05$).

$GABA_A$ receptor-binding sites were labeled with [^{3}H]muscimol (mean density 1,810 ± 188 fmol/mg protein). Since binding increased medial to NCC, the border of the NCL could be easily visualized (Fig. 1a/b). The Friedman ANOVA showed a significant main effect [Chi Square ($N = 6$, df $= 2$) $= 12$, $p < 0.005$]. Subsequent Wilcoxon tests revealed a significantly stepwise decrease of binding from NCC over NCL to CDL (all $N = 6$, $T = 0$, $p < 0.05$) that is particularly illustrated in the fingerprints (Fig. 2a).

The study of binding sites for the neurotransmitter acetylcholine revealed low densities for all analyzed cholinergic receptors. Binding of [^{3}H]pirenzepine to muscarinergic cholinergic receptors of the M_1-type was very low in the caudolateral nidopallium (NCL: 151 ± 24 fmol/mg protein; Figs. 1a/b, 2a). A further differentiation within NCL was not visible. The Friedman ANOVA using the data from NCL, NCC and CDL showed a significant overall effect [Chi Square ($N = 6$, df $= 2$] $= 6.52$, $p < 0.05$). Subsequent Wilcoxon tests revealed that the concentration was significantly lower in NCL compared to both NCC and CDL ($N = 6$, $T \leq 1$, $p < 0.05$; Fig. 2).

M_2-receptors presented the highest densities of all determined cholinergic receptors in the nidopallial structures (269 ± 39 fmol/mg protein; Fig. 2a). The Friedman ANOVA comparing NCL, NCC and CDL showed a significant overall effect [Chi Square ($N = 6$, df $= 2$) $=$ 10.33, $p < 0.01$). Subsequent Wilcoxon tests revealed a

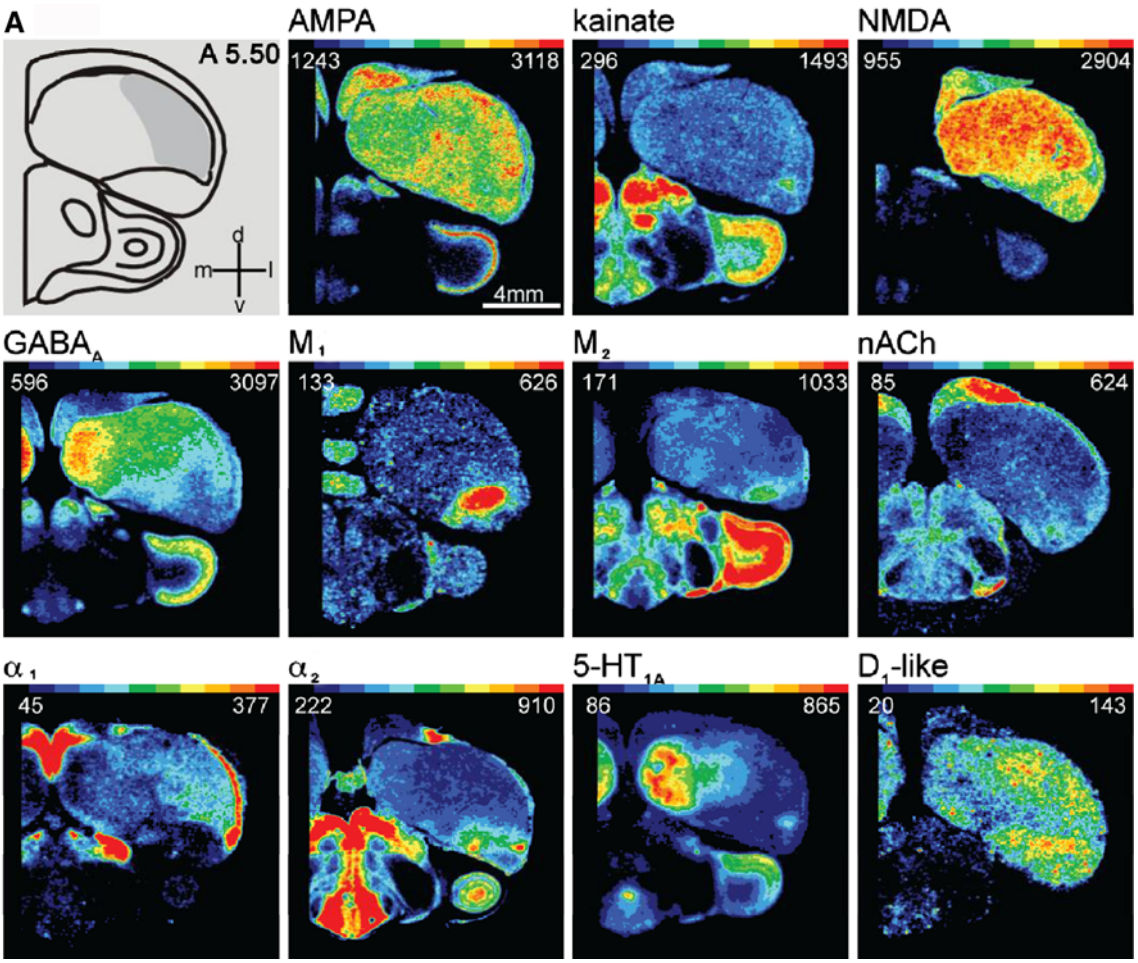

Fig. 1 Color-coded autoradiographs showing the distribution of AMPA, kainate, NMDA, $GABA_A$, M_1, M_2, nicotinic cholinergic (nACh), α_1, α_2, 5-HT_{1A} and D_1-like receptors in coronal sections through the pigeon brain at rostrocaudal levels A 5.50 (**a**) and A 6.75 (**b**). Extent of the NCL at each of these levels is highlighted in gray in the schematic drawing. *Scale bars* code for receptor densities in fmol/mg protein

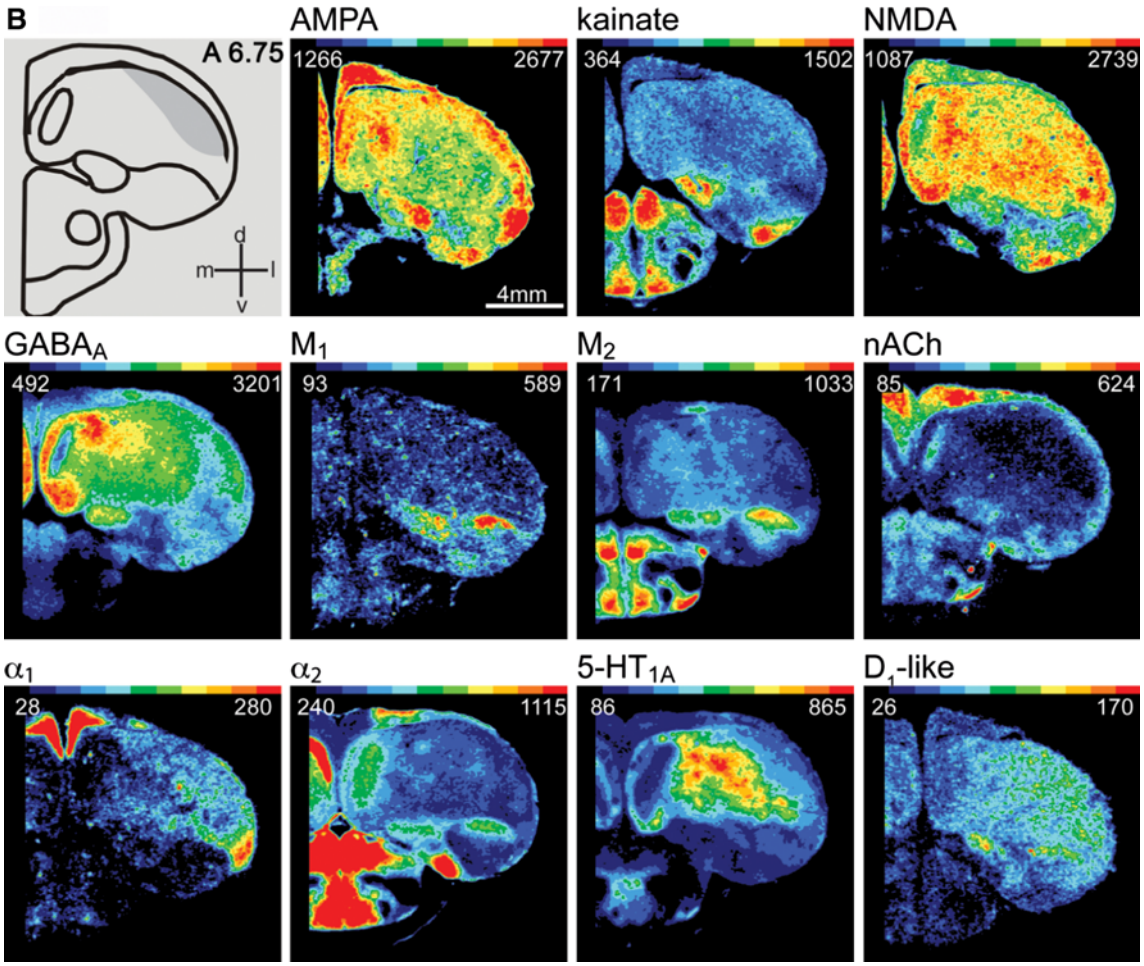

Fig. 1 continued

significantly stepwise increase of binding strength from CDL over NCL to NCM ($N = 6$, $T \leq 1$, $p < 0.05$) and a parcellation of NCLm and NCLl ($N = 6$, $T = 0$, $p < 0.05$; Fig. 3).

Binding of [^{3}H]cytisine to nicotinic receptors was very low in the whole lateral aspect of the nidopallium (144 ± 12 fmol/mg protein, Fig. 1a/b and Fig. 2a), indicating low densities of nACh receptors (Fig. 2a). The Friedman ANOVA showed a significant overall effect [Chi Square ($N = 6$, df $= 2$) $= 12$, $p < 0.005$]. Subsequent Wilcoxon tests revealed a significantly stepwise decrease of binding strength from CDL over NCL to NCC ($N = 6$, $T = 0$, $p < 0.05$). Further, binding densities between NCLm and NCLl differed significantly ($N = 6$, $T = 0$, $p < 0.05$; Fig. 3).

The noradrenergic α_1 receptor was visualized by means of [^{3}H]prazosin (127 ± 16 fmol/mg protein; Fig. 1a/b). Although in few cases the ventral aspect of the NCL, abutting the arcopallium, displayed some higher binding, this was not consistently observed. A differentiation between NCLl and NCLm was not evident. The Friedman ANOVA comparing NCL, NCC and CDL showed a significant overall effect [Chi Square ($N = 6$, df $= 2$) $= 12$, $p < 0.005$]. Subsequent Wilcoxon tests revealed a significantly stepwise decrease of binding strength from CDL over NCL to NCC (all $N = 6$, $T = 0$, $p < 0.05$; Fig. 2a).

[^{3}H]RX821002 binds to noradrenergic α_2 receptor and displayed moderate binding in NCL (308±27 fmol/mg protein). Substructures within the NCL were not visible (Fig. 1a/b). The Friedman ANOVA showed a significant overall effect [Chi Square ($N = 6$, df $= 2$) $= 9.33$, $p < 0.01$]. Subsequent Wilcoxon tests revealed that binding in NCC was significantly higher than both in NCL and CDL (all $N = 6$, $T = 0$, $p < 0.05$; Fig. 2).

Serotonergic 5-HT$_{1A}$ receptor-binding sites were visualized with [^{3}H]8-OH-DPAT. NCL revealed lower densities (374 ± 67 fmol/mg protein) than the medially abutting nidopallial areas, again providing the possibility to clearly identify the medial wall of the NCL (Fig. 1a/b). The Friedman ANOVA showed a significant overall effect

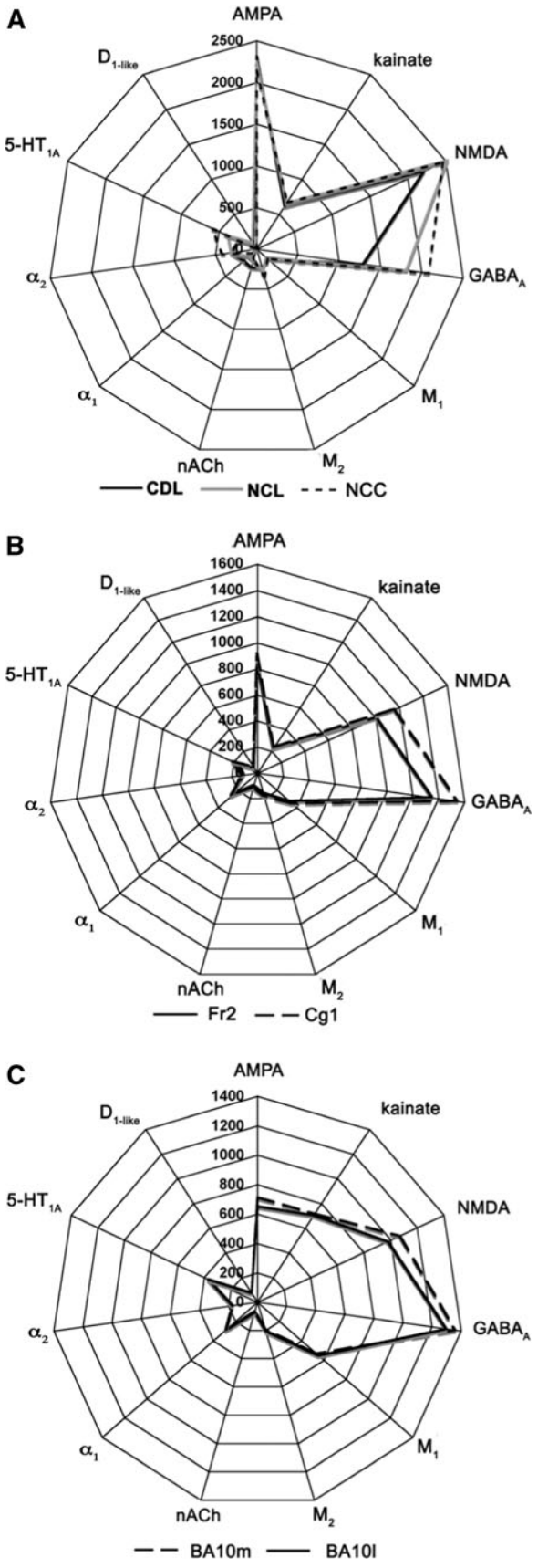

◀ **Fig. 2** Receptor fingerprints for CDL, NCL, NCC of the pigeon pallium (**a**), for Fr2 and Cg1 of the rat cortex (**b**) and for the BA10l and BA10m of the human cortex (**c**). The mean densities (fmol/mg protein) of glutamatergic (AMPA, kainate, NMDA), GABAergic ($GABA_A$), acetylcholinergic muscarinic (M_1, M_2) and nicotinic (nACh), adrenergic (α_1, α_2), serotonergic ($5\text{-}HT_{1A}$) and dopaminergic (D_1-like) receptors are displayed in polar coordinate plots. The lines connecting the mean densities define the shape of the fingerprint based on 11 different binding sites for each area. Note that the scales in **a**–**c** are different. *BA10l* Brodmann area 10 lateral, *BA10m* Brodmann area 10 medial, *CDL* area corticoidea dorsolateralis, *NCL* nidopallium caudolaterale, *NCC* nidopallium caudocentrale, *Fr2* frontal area 2, *Cg1* cingulate cortex 1

[Chi Square ($N = 6$, df $= 2$] $= 12$, $p < 0.005$). Subsequent Wilcoxon tests revealed a significantly stepwise increase of binding strength from CDL over NCL to NCC (all $N = 6$, $T = 0$, $p < 0.05$, Fig. 2a). Furthermore, $5\text{-}HT_{1A}$ receptors were more abundant in NCLm than NCLl ($N = 6$, $T = 0$, $p < 0.05$; Fig. 3).

[^{3}H]SCH23390 was used to reveal the location and density of dopaminergic D_1-like receptors. Ligand binding was mainly concentrated within the NCL without showing a difference between the lateral and the medial component (Fig. 1a/b). Although density in NCL was rather low (92 ± 12 fmol/mg protein), a Friedman ANOVA comparing NCL, NCC, and CDL showed a significant overall effect [Chi Square ($N = 6$, df $= 2$) $= 12$, $p < 0.01$]. A subsequent Wilcoxon test revealed significantly higher values for NCL and CDL over NCC ($N = 6$, $T = 0$, $p < 0.05$; Fig. 2) as well as significantly higher values for NCL than for CDL ($N = 6$, $T = 0$, $p < 0.05$; Fig. 2).

Based on the different binding site densities for kainate, NMDA, $GABA_A$, M_1, M_2, nACh, α_1, α_2, $5\text{-}HT_{1A}$ and D_1-like receptors a detailed outline of the NCL is depicted in Fig. 4.

Comparison of receptor-binding site densities in the avian NCL to mammalian prefrontal structures

In the rat (Fig. 2b) and human (Fig. 2c) prefrontal areas examined, AMPA and $GABA_A$ receptors showed the highest densities of all measured receptor types, and were followed by NMDA receptor densities (Fig. 2b/c). Lowest values were found for nACh, and D_1-like receptor densities.

Human and rat prefrontal areas differed considerably in their relative balance of ionotropic glutamatergic receptors. In human areas, BA10l and BA10m, kainate receptor densities were comparable to those of AMPA receptors, and only slightly lower than those of NMDA receptors (Fig. 2c). In rat areas, Fr2 and Cg1, similar to the situation described for the pigeon nidopallial areas, kainate receptor

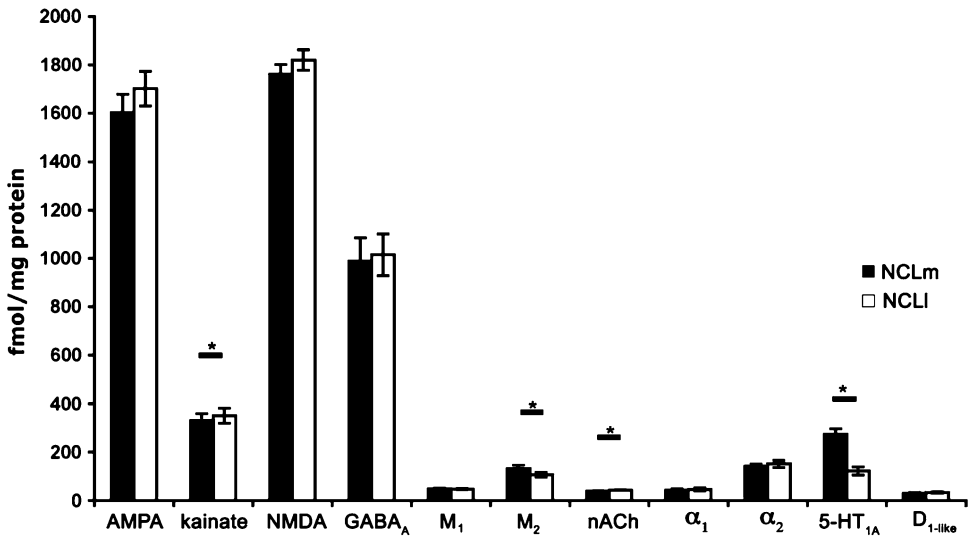

Fig. 3 Histogram of the mean receptor densities (fmol/mg protein) of the pigeon's areas NCLm and the NCLl. *Error bars* represent standard deviations. *Asterisks* indicate significant differences between receptor densities

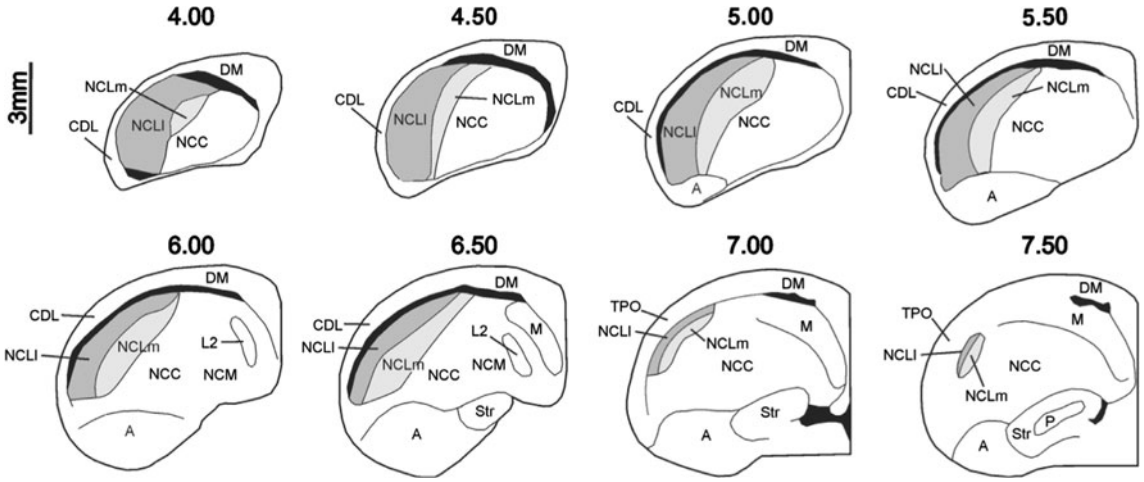

Fig. 4 Atlas of the NCL in serial frontal sections based on different receptor densities. The length of the bar represents 3 mm

densities were considerably lower than those of AMPA (fourfold lower) or NMDA (five to sixfold lower) receptor densities (Fig. 2b). Thus, the pigeon and rat, but not the human fingerprints presented a conspicuous indentation at the level of the kainate receptors.

The examined human and rat prefrontal areas presented the same balance of cholinergic receptor densities, with highest concentrations for the muscarinic M_1 cholinergic type and lowest values for the nicotinic receptor (Fig. 2b/c). This pattern differs however, from that of pigeons, since nidopallial areas contain higher M_2 than M_1 receptor densities (Fig. 2a).

In the group of monoaminergic receptors, noradrenergic α_1 receptor densities were higher than those of α_2 receptors in both human and rat prefrontal areas (Fig 2b/c). Conversely, α_1 receptor densities were lower than of α_2 receptor densities in the pigeon nidopallium (Fig. 2a). Serotoninergic 5-HT_{1A} receptor densities were higher than those of α_1 receptors in human areas BA10l and BA10m, whereas the opposite holds true for rat areas Fr2 and Cg1 (Fig. 2b/c). D_1-like binding-site densities showed neither differences between the analyzed prefrontal structures nor the pigeon's NCL (Fig. 2b/c).

Discussion

Using a quantitative analysis of 11 different receptor-binding sites, the present study aimed to (1) analyze the areal borders of the constituents of the caudolateral part of the pigeons' telencephalon, (2) to reveal possible subdivisions within the NCL, (3) to compare the receptor fingerprints of NCL and the surrounding NCC and CDL with those of frontal areas in mammals.

Areal delineation in the pigeons' caudolateral telencephalon

Moving from centromedial to lateral, the avian caudolateral telencephalon is constituted by the three areas: NCC, NCL, and CDL. The NCC receives its input predominantly from the dorsal intermediate mesopallium and projects to arcopallial subfields. The arcopallial outflow to the medial hypothalamus could imply that NCC is involved in neuroendocrine and autonomic functions and is limbic in nature (Yamamoto and Reiner 2005; Atoji and Wild 2009). The interconnectivity between NCC and NCL seems to be surprisingly weak (Atoji and Wild 2009; Kröner and Güntürkün 1999). Further, the pattern of afferents and efferents of NCC and NCL is considerably different (Leutgeb et al. 1996; Metzger et al. 1998; Kröner and Güntürkün 1999; Atoji and Wild 2009). Thus, although NCC and NCL cannot be delineated by cytoarchitectonic means and were subsumed into area Ne16 in the quantitative cytoarchitectonic study of Rehkämper and Zilles (1991), they show marked differences in hodology. The study of Atoji and Wild (2009) placed the borderline between NCC and NCL far more laterally than the immunocytochemical and connectivity analyses conducted on the NCL (Waldmann and Güntürkün 1993; Leutgeb et al. 1996; Kröner and Güntürkün 1999; Riters et al. 1999). In fact, according to Atoji and Wild (2009), NCLm would be part of NCC. Interestingly, the reconstruction of the location of retrogradely labeled neurons in Atoji and Wild (2009) reveals a border that is more close to that of the present study and similar to the original delineation by Waldmann and Güntürkün (1993) and this is reflected by the distribution patterns of α_1, 5-HT_{1A} and D_1-like receptors. However, the caudal aspect of the avian nidopallium is organized in clusters with fuzzy borders; in addition, not all receptor-binding sites defined clear boundaries between areas. Thus, the distribution patterns of the receptors confirm a smooth transition at the caudal site and both areas probably do not have a clear boundary at that point. Therefore, in the most caudal portion of the nidopallium, the delineation between NCC and NCL becomes extremely difficult and may have led to different findings in the past (Atoji and Wild 2009).

Towards the lateral border, the distinction between NCL and CDL is easy due to the ventricle that separates these two areas. The CDL is considered to be mostly limbic in nature and was hodologically compared to the mammalian cingulate cortex (Yamamoto and Reiner 2005; Atoji and Wild 2005; Csillag and Montagenese 2005). It shares similarities with the receptor architecture of the hippocampal formation (data not shown) and nidopallial structures. CDL extents rostrally up to A 6.75 where NCL and CDL are no longer separated by the lateral ventricle but directly abut each other. At this point, the autoradiographic data revealed a less fuzzy transition when compared to the caudal aspects of NCL and NCC, depicting that NCL follows the outer curvature of the telencephalon but always stays about 1 mm away from the pial surface. Similarly, the rostral border of the NCL is easier to define as it tapers up to A 7.50.

Subdivisions of the NCL

Our findings reveal a clear parcellation of the avian nidopallium that is in line with tracing studies (Rehkämper and Zilles 1991; Leutgeb et al. 1996; Kröner and Güntürkün 1999; Atoji and Wild 2009). Earlier studies have shown functional and neurochemical subdivisions of the NCL (Leutgeb et al. 1996; Braun et al. 1999; Kröner and Güntürkün 1999; Riters et al. 1999). Here, a new subdivision into a medial and a lateral part is proposed by the differences of the mean receptor densities of nACh, M_2, kainate, and 5-HT_{1A} receptors. Some earlier tracing and neurochemical studies revealed a possible dorsal and ventral component (Leutgeb et al. 1996; Braun et al. 1999; Riters et al. 1999). The neurochemical subdivision into a dorsal and a ventral component also coincides with hodological data showing that only dorsal NCL receives afferents from multimodal thalamic nuclei (Korzeniewska and Güntürkün 1990; Güntürkün and Kröner 1999) and contributes more significantly to working memory performance (Diekamp et al. 2002a, b). Dorsal, but not ventral NCL, is connected with a complex of association structures in the rostromedial nidopallium and ventral hyperpallium in different species of birds. In domestic chicken two extensively overlapping structures, the mediorostral nidopallium/hyperpallium (MNH) and the intermediate and medial mesopallium ventrale (IMM), play a pivotal role in auditory and visual filial imprinting, respectively (Horn 1981; Braun et al. 1999). These areas are activated during imprinting and lesions cause deficits in recognizing the imprinting stimulus (Horn 1981; Horn et al. 1985). In chicken, IMM is also a nodal point of initial memory formation in one-trial passive avoidance learning with gustatory cues (Rose 2000). Both MNH and IMM project to dorsomedial NCL as shown in chicken (Metzger et al. 1998) and pigeons (Kröner and Güntürkün 1999). However, we could not confirm a border between dorsal and ventral NCL based on the receptor-density profiles. On the other hand, Kröner and Güntürkün (1999) demonstrated that the component labeled NCLl in our preparations receives input from secondary areas of sensory representation and projects back to these structures. Furthermore, a large number of neurons from NCL projects to the arcopallium and these output neurons are close to the densest catecholaminergic innervations that are located in the

lateral part of the NCL (Waldmann and Güntürkün 1993; Kröner and Güntürkün 1999). In addition, a large number of medial NCL neurons project to the basal ganglia in pigeons (Veenman et al. 1995; Kröner and Güntürkün 1999). Therefore, NCLl displayed a different connectivity pattern from NCLm. Due to the curvature of the NCL, NCLl is positioned more dorsally than NCLm. Thus, a dorsoventral subdivision of the NCL could mistakenly be concluded from the lateromedial differentiation of a semilunar structure.

The neurochemistry of the caudolateral avian forebrain

In NCL, NCC, and CDL the highest receptor densities were detected for glutamatergic and $GABA_A$ receptors. This is in line with earlier studies that determined receptor levels in the nidopallium of various bird species (Dietl and Palacios 1988; Stewart et al. 1988,1999; Mitsacos et al. 1990; Aamodt et al. 1992; Veenman et al. 1994; Ben-Ari et al. 1997; Salvatierra et al. 1997). Pigeons showed higher AMPA and NMDA receptor concentrations in the nidopallium when compared to other birds, while the amount of $GABA_A$ receptor densities seemed to be similar in pigeons, chicks and zebra finches (Stewart et al. 1988; Henley and Barnard 1990; Veenman et al. 1994; Martinez de la Torre et al. 1998; Stewart et al. 1999; Pinaud and Mello 2007). The present study reports for the first time kainate receptor densities in the pigeon's pallium. If compared to AMPA and NMDA receptors, kainate binding was about four times lower in all of the above-mentioned structures. However, like for the NMDA receptors, kainate binding differed between the CDL and the nidopallial structures, showing a clear segregation. This is in line with an immunohistochemical study in quails, showing that AMPA and NMDA receptors have higher densities than kainate receptors in the nidopallium. In addition, kainate and NMDA binding is lower in the CDL while the AMPA receptor subunit GluR1 was intensely labeled in the CDL (Cornil et al. 2000). Binding of the $GABA_A$ receptor also increased from the surface to the deeper nidopallial areas, confirming earlier immunohistochemical und receptor autoradiographic studies (Rehkämper and Zilles 1991; Veenman et al. 1994). In the nidopallium, cholinergic muscarinic and nicotinic receptors showed an intermediate to low density, which is in line with results from other studies of muscarinic or nicotinic binding sites in the telencephalon of pigeons, chicks, quails, sparrows, and starlings (Dietl et al. 1988; Ball et al. 1990; Sorenson and Chiappinelli 1992). As described for the $GABA_A$ receptor, the M_2 receptor density increases from the superficial CDL over the NCL to the NCM while the nACh receptor densities decreases. The boundaries of the NCL were revealed by all cholinergic receptors.

The monoaminergic receptors were differentially distributed. Their densities ranged from very low (D_1-like receptors) to moderate (5-HT_{1A} receptors). Densities of the α_2 receptors varied across different bird species in the CDL and in the nidopallium (Balthazart and Ball 1989; Ball et al. 1995; Diez-Alarcia et al. 2006). To our knowledge to date no specific information about the densities of 5-HT_{1A} receptor densities is available on the avian pallium, although it was shown in a competition assay with [^{3}H]5-HT binding that 5-HT_{1A} receptors were abundant in the pigeon's telencephalon (Waeber et al. 1989). Comparable results were reported for the D_1-like receptor in the nidopallium of pigeons (Dietl and Palacios 1988).

Comparison to mammals and functional considerations

As first shown by lesion experiments (Mogensen and Divac 1982), the NCL is involved in executive functions. More recent studies have confirmed that the NCL shares many similarities with the mammalian prefrontal cortex (Güntürkün, 2005a, b; Kirsch et al. 2008). These findings can be seen in parallel to observations in corvids and parrots which possess cognitive abilities that are comparable to those of monkeys and apes (Bird and Emery 2010; Hunt and Gray 2003; Emery and Clayton 2004; Kenward et al. 2005; Seed et al. 2006; Prior et al. 2008; Taylor et al. 2009; Pollok et al., 2000). As observed for other mammals (Harvey and Krebs 1990) this is accompanied by an increased encephalization (Cnotka et al. 2008) and a relative growth of associative forebrain areas (Mehlhorn et al. 2010). Based on topographical and genetic arguments both the NCL and the prefrontal cortex seem to be a case of homoplasy (Puelles et al. 2000). Additionally, the morphological organization of avian and mammalian forebrains differs importantly, with the avian pallium having a nuclear organization while the mammalian dorsal pallium assumes a laminar structure. Thus, a layered cortical structure appears not to be a prerequisite for higher cognitive functions (Kirsch et al. 2008). In contrast to the NCL, less is known about the CDL and its functions. The connections of the avian CDL share similarities with those of the mammalian cingulate cortex (Vogt and Pandya 1987; Atoji and Wild 2005). Neurobehavioral studies in which the CDL was lesioned as part of larger lesions to the lateral nidopallium or the hippocampal formation indicate a role for the CDL in spatial memory (Hartmann and Güntürkün 1998; Bingman et al. 1985; Colombo et al. 2001; Gagliardo et al. 2001). Only one study showed that CDL lesions did not impair performance in simultaneous pattern or delayed alternation discrimination tasks (Gagliardo et al. 1996). Receptor autoradiography and receptor fingerprints of brain regions provide a tool to compare the chemoarchitecture between different species.

Therefore, our results will be further discussed in the light of comparative studies in birds, primates and rats.

As in the pigeon's NCL and CDL, high receptor densities for glutamatergic and GABAergic receptors were found in the prefrontal regions investigated here, as well as in other cortical regions of rats, monkeys and humans (Gebhard et al. 1995; Geyer et al. 1998; Zilles et al. 2002a, b; Palomero-Gallagher and Zilles 2004). However, there were differences in the amount of distinct glutamate receptors between species. AMPA and NMDA receptors showed high concentrations in the NCL and the CDL of pigeons and chicks (Bock et al. 1997) if compared to frontal structures of mammals. Kainate receptors seemed to be very low in rat FR2 and Cg1, while they did not differ substantially between human BA10 and the NCL, and between the CDL and the human cingulate cortex (Palomero-Gallagher et al. 2009). By contrast, the amounts of $GABA_A$ receptors were equally distributed in the prefrontal areas of all the investigated species here and also in the NCL of pigeons and chicks (Stewart et al. 1988). The same is true for the CDL and the human as well as the macaque cingulate cortex (Bozkurt et al. 2005; Palomero-Gallagher et al. 2009). Thus, there seems to be a shift towards higher densities of glutamate receptors in avian nidopallial structures. Therefore, the top right quadrant of the fingerprints for the birds' nidopallial structures differs in size when compared to the rodent frontal areas, and differ in shape for both species, if compared to human BA10.

Cholinergic M_1 receptors were highest in human if compared to macaque monkey, rhesus monkey, rat and pigeon, while M_2 and nicotinic receptors showed equal densities (Bozkurt et al. 2005; Lidow et al. 1989). However, pigeons showed an inverted pattern of M_1/M_2 binding if compared to other species. ACh is an essential regulator of cortical excitability and plays important roles for arousal, attention, and cognitive processes (Sarter and Bruno 2000; Hasselmo and Stern 2006; Briand et al. 2007; Sarter et al. 2009). These functions are mediated by muscarinic and nicotinic ACh receptors. In the cerebral cortex the M_1 receptor is preferentially expressed in pyramidal cells and enriched on the extrasynaptic membrane of their dendrites and spines (Yamasaki et al. 2010). The M_2 receptor is the primary muscarinic autoreceptor presynaptically regulating ACh release in the forebrain of rodents and primates including humans (Mrzljak et al. 1995; Zhang et al. 2002). Both receptor subtypes are metabotropic. M_1 couples to a stimulatory G-protein whereas M_2 couples to an inhibitory G-protein. Genetic variation of the CHRM2 gene encoding the M_2 receptor selectively influence muscarinic presynaptic inhibition (Comings et al. 2003). The nACh receptors are fast-acting ligand-gated ion channels producing EPSPs. A recent genetic approach showed that both, fast-acting nicotinic receptors and slow-acting muscarinic receptors influence in a synergistic system the efficiency of shifting visuospatial attention in the PFC (Greenwood et al. 2009). In pigeons, central cholinergic systems are important for temporal memory processes and spatial orientation during homing, two processes that also involve the NCL (Gagliardo and Divac 1993; Santi and Weise 1995; Kohler et al. 1996; Riters and Bingman 1999).

Like for the muscarinic cholinergic receptors, the same inverted ratio was detected in the NCL and in the CDL for the noradrenergic α_1 and α_2 receptors if compared to prefrontal or cingulate structures in mammals. In humans, macaque monkeys and rats higher amounts of α_1 than of α_2 receptors were described (Goldman-Rakic et al. 1990; Bozkurt et al. 2005; Palomero-Gallagher et al. 2009). Both receptor types are metabotropic and α_1 receptors are coupled to stimulatory G-proteins, while α_2 receptors are coupled to inhibitory G-proteins. In the PFC of monkeys, α_2 receptors are located postsynaptically at the dendritic spines of pyramidal neurons where glutamate receptors are concentrated (Aoki et al. 1998). Behavioral pharmacological studies in rodents, monkeys, and humans demonstrated that systemically or locally administered α_2 receptor agonists could improve PFC cognitive performances (Robbins and Arnsten 2009). Further, it was shown that stimulation of α_2 receptors suppresses glutamate synaptic transmission in the PFC and tunes the synaptic output to an optimal state for working memory function (Wang et al. 2007; Ji et al. 2008). In songbirds noradrenalin is involved in song learning at different developmental stages by controlling local circuits in the higher vocal center (HVC) (Fortune and Margoliash 1995) and modulation of auditory responses through attention processes (Castelino and Schmidt 2010). The HVC could be an oscine specialization of the dorsal NCL (Farries 2001). Because both the M_1/M_2 and the α_1/α_2 ratio show an inverted pattern in the NCL resulting in an increased inhibitory control on local circuits this may be a compensating mechanism for the shift to glutamatergic processing.

The densities of 5-HT_{1A} receptors were equal in the prefrontal areas of humans, monkeys and pigeons, while rats showed lower densities (Goldman-Rakic et al. 1990). The 5-HT_{1A} subtype is of particular interest, since it is one of the main mediators of 5-HT and contributes to a lot of prefrontal functions (Sakaue et al. 2000; de Almeida et al. 2008). In the human cingulate cortex the density of the 5-HT_{1A} subtype is slightly higher than in the CDL (Palomero-Gallagher et al. 2009). In birds less is known about the serotonergic contribution to executive functions, but it was shown that serotonin release was increased in the NCL during a working memory task (Karakuyu et al. 2007).

D_1-like receptors showed the lowest densities of all measured receptor types in the assumed prefrontal and cingulate regions of pigeons, rats, monkeys, cats, tree

shrews and humans (Richfield et al. 1989; Goldman-Rakic et al. 1990; Palomero-Gallagher et al. 2009). In mammals, low densities of D_1-like receptors in frontal areas are associated with volume transmission of dopamine and a diffuse action of dopamine on multiple components of cortical networks (reviewed in Gonzalez-Burgos et al. 2007). These results also reveal that the dopaminergic system seems to be highly conserved across species, although prefrontal structures evolved independently (Callier et al. 2003). Thus, the dopaminergic system and its interactions with other systems might constitute a key element for our understanding of the anatomical/chemical traits that are necessary for proper executive functions. The low density of D_1-like receptors might also explain why species share similar deficits if signaling via this receptor-type is disturbed (Zahrt et al. 1997; Williams and Castner 2006; Herold et al. 2008; McNab and Klingberg 2008; Rose et al. 2010).

In summary, it appears that the GABAergic and dopaminergic systems are highly conserved across the species studied here, which have a long history of separate evolution (Jarvis et al. 2005). This could result from a common selection pressure for a structure that serves executive functions, i.e., the control of higher order processes. This includes the integration and manipulation of information from all modalities in order to generate a proper behavior in a given situation. These functions rely on specific connections to other brain structures and the modulation of information flow through these circuits. Thus, similar evolutionary pressures on information processing in birds might result in a comparable or analogue pattern of specific receptor compositions that would resemble those in the neocortex of mammals. Future studies need to examine differences between various bird species, as well as between different mammalian species to confirm these conclusions.

Acknowledgments Supported by a grant from the BMBF through the Bernstein Focus Group "Varying Tunes" to O.G.

Conflict of interest The authors declare that they have no conflict of interest.

References

Aamodt SM, Kozlowski MR, Nordeen EJ, Nordeen KW (1992) Distribution and developmental change in [3H]MK-801 binding within zebra finch song nuclei. J Neurobiol 23:997–1005

Amunts K, Weiss PH, Mohlberg H, Pieperhoff P, Eickhoff S, Gurd JM, Marshall JC, Shah JN, Fink GR, Zilles K (2004) Analysis of the neural mechanisms underlying verbal fluency in cytoarchitectonically defined stereotaxic space—the roles of Brodmann areas 44 and 45. NeuroImage 22:42–56

Amunts K, Schleicher A, Zilles K (2007) Cytoarchitecture of the cerebral cortex—more than localization. NeuroImage 37:1061–1065

Aoki C, Venkatesan C, Go CG, Forman R, Kurose H (1998) Cellular and subcellular sites for noradrenergic action in the monkey dorsolateral prefrontal cortex as revealed by the immunocytochemical localization of noradrenergic receptors and axons. Cereb Cortex 8:269–277

Atoji Y, Wild JM (2005) Afferent and efferent connections of the dorsolateral corticoid area and a comparison with connections of the temporo-parieto-occipital area in the pigeon (*Columba livia*). J Comp Neurol 485:165–182

Atoji Y, Wild JM (2009) Afferent and efferent projections of the central caudal nidopallium in the pigeon (*Columba livia*). J Comp Neurol 517:350–370

Ball GF, Nock B, Wingfield JC, McEwen BS, Balthazart J (1990) Muscarinic cholinergic receptors in the songbird and quail brain: a quantitative autoradiographic study. J Comp Neurol 298:431–442

Ball GF, Casto JM, Balthazart J (1995) Autoradiographic localization of D1-like dopamine receptors in the forebrain of male and female Japanese quail and their relationship with immunoreactive tyrosine hydroxylase. J Chem Neuroanat 9:121–133

Balthazart J, Ball GF (1989) Effects of the noradrenergic neurotoxin DSP-4 on luteinizing hormone levels, catecholamine concentrations, alpha 2-adrenergic receptor binding, and aromatase activity in the brain of the Japanese quail. Brain Res 492:163–175

Bast T, Diekamp B, Thiel C, Schwarting RK, Güntürkün O (2002) Functional aspects of dopamine metabolism in the putative prefrontal cortex analogue and striatum of pigeons (*Columba livia*). J Comp Neurol 446:58–67

Ben-Ari Y, Khazipov R, Leinekugel X, Caillard O, Gaiarsa JL (1997) GABAA, NMDA and AMPA receptors: a developmentally regulated 'menage a trois'. Trends Neurosci 20:523–529

Bingman VP, Ioalè P, Casini G, Bagnoli P (1985) Dorsomedial forebrain ablations and home loft association behavior in homing pigeons. Brain Behav Evol 26:1–9

Bird CD, Emery NJ (2010) Rooks perceive support relations similar to six-month-old babies. Proc Biol Sci 277:147–151

Bock J, Schnabel R, Braun K (1997) Role of the dorso-caudal neostriatum in filial imprinting of the domestic chick: a pharmacological and autoradiographical approach focused on the involvement of NMDA-receptors. Eur J Neurosci 9:1262–1272

Bozkurt A, Zilles K, Schleicher A, Kamper L, Arigita ES, Uylings HB, Kötter R (2005) Distributions of transmitter receptors in the macaque cingulate cortex. Neuroimage 25:219–229

Braun K, Bock J, Metzger M, Jiang S, Schnabel R (1999) The dorsocaudal neostriatum of the domestic chick: a structure serving higher associative functions. Behav Brain Res 98:211–218

Briand LA, Gritton H, Howe WM, Young DA, Sarter M (2007) Modulators in concert for cognition: modulator interactions in the prefrontal cortex. Prog Neurobiol 83:69–91

Brodmann K (1909) Vergleichende Lokalisationslehre der Großhirnrinde in ihren Prinzipien dargestellt auf Grund des Zellenbaues, Barth, Leipzig; English translation available in Garey, L. J. Brodmann's Localization in the Cerebral Cortex (Smith Gordon, London, 1994)

Callier S, Snapyan M, Le Crom S, Prou D, Vincent JD, Vernier P (2003) Evolution and cell biology of dopamine receptors in vertebrates. Biol Cell 95:489–502

Castelino CB, Schmidt MF (2010) What birdsong can teach us about the central noradrenergic system. J Chem Neuroanat 39:96–111

Cnotka J, Güntürkün O, Rehkämper G, Gray RD, Hunt GR (2008) Extraordinary large brains in tool-using New Caledonian crows (*Corvus moneduloides*). Neurosci Lett 433:241–245

Colombo M, Broadbent NJ, Taylor CS, Frost N (2001) The role of the avian hippocampus in orientation in space and time. Brain Res 919:292–301

Comings DE, Wu S, Rostamkhani M, McGue M, Lacono WG, Cheng LS, MacMurray JP (2003) Role of the cholinergic muscarinic 2 receptor (CHRM2) gene in cognition. Mol Psychiatry 8:10–11

Cornil C, Foidart A, Minet A, Balthazart J (2000) Immunocytochemical localization of ionotropic glutamate receptors subunits in the adult quail forebrain. J Comp Neurol 428:577–608

Csillag A, Montagnese CM (2005) Thalamotelencephalic organization in birds. Brain Res Bull 66:303–310

de Almeida J, Palacios JM, Mengod G (2008) Distribution of 5-HT and DA receptors in primate prefrontal cortex: implications for pathophysiology and treatment. Prog Brain Res 172:101–115

Diekamp B, Kalt T, Güntürkün O (2002a) Working memory neurons in pigeons. J Neurosci 22:RC210

Diekamp B, Gagliardo A, Güntürkün O (2002b) Nonspatial and subdivision-specific working memory deficits after selective lesions of the avian prefrontal cortex. J Neurosci 22:9573–9580

Dietl MM, Palacios JM (1988) Neurotransmitter receptors in the avian brain. I. Dopamine receptors. Brain Res 439:354–359

Dietl MM, Cortes R, Palacios JM (1988) Neurotransmitter receptors in the avian brain. II. Muscarinic cholinergic receptors. Brain Res 439:360–365

Diez-Alarcia R, Pilar-Cuellar F, Paniagua MA, Meana JJ, Fernandez-Lopez A (2006) Pharmacological characterization and autoradiographic distribution of alpha2-adrenoceptor antagonist [3H]RX 821002 binding sites in the chicken brain. Neuroscience 141:357–369

Divac I, Mogensen J, Bjorklund A (1985) The prefrontal 'cortex' in the pigeon. Biochemical evidence. Brain Res 332:365–368

Durstewitz D, Kröner S, Hemmings HC Jr, Güntürkün O (1998) The dopaminergic innervation of the pigeon telencephalon: distribution of DARPP-32 and co-occurrence with glutamate decarboxylase and tyrosine hydroxylase. Neuroscience 83:763–779

Eickhoff S, Amunts K, Mohlberg H, Zilles K (2006) The human parietal operculum. II. Stereotaxic maps and correlation with functional imaging results. Cereb Cortex 16:268–279

Emery NJ, Clayton NS (2004) The mentality of crows: convergent evolution of intelligence in corvids and apes. Science 306:1903–1907

Farries MA (2001) The oscine song system considered in the context of the avian brain: lessons learned from comparative neurobiology. Brain Behav Evol 58:80–100

Fortune ES, Margoliash D (1995) Parallel pathways and convergence onto HVc and adjacent neostriatum of adult zebra finches (*Taeniopygia guttata*). J Comp Neurol 360:413–441

Gagliardo A, Divac I (1993) Effects of ablation of the presumed equivalent of the mammalian prefrontal cortex on pigeon homing. Behav Neurosci 107:280–288

Gagliardo A, Bonadonna F, Divac I (1996) Behavioural effects of ablations of the presumed 'prefrontal cortex' or the corticoid in pigeons. Behav Brain Res 78:155–162

Gagliardo A, Ioalè P, Odetti F, Bingman VP, Siegel JJ, Vallortigara G (2001) Hippocampus and homing in pigeons: left and right hemispheric differences in navigational map learning. Eur J Neurosci 13:1617–1624

Gebhard R, Zilles K, Schleicher A, Everitt BJ, Robbins TW, Divac I (1995) Parcellation of the frontal cortex of the New World monkey *Callithrix jacchus* by eight neurotransmitter-binding sites. Anat Embryol (Berl) 191:509–517

Geyer S, Matelli M, Luppino G, Schleicher A, Jansen Y, Palomero-Gallagher N, Zilles K (1998) Receptor autoradiographic mapping of the mesial motor and premotor cortex of the macaque monkey. J Comp Neurol 397:231–250

Goldman-Rakic PS (1999) The "psychic" neuron of the cerebral cortex. Ann N Y Acad Sci 868:13–26

Goldman-Rakic PS, Lidow MS, Gallager DW (1990) Overlap of dopaminergic, adrenergic, and serotoninergic receptors and complementarity of their subtypes in primate prefrontal cortex. J Neurosci 10:2125–2138

Gonzalez-Burgos G, Kröner S, Seamans JK (2007) Cellular mechanisms of working memory and its modulation by dopamine in the prefrontal cortex of primates and rats. In: Tseng KY, Atzori M (eds) Monoaminergic Modulation of Cortical Excitability. Springer, Berlin, pp 125–152

Greenwood PM, Lin MK, Sundararajan R, Fryxell KJ, Parasuraman R (2009) Synergistic effects of genetic variation in nicotinic and muscarinic receptors on visual attention but not working memory. Proc Natl Acad Sci USA 106:3633–3638

Güntürkün O (1997) Cognitive impairments after lesions of the neostriatum caudolaterale and its thalamic afferent: functional similarities to the mammalian prefrontal system? J Brain Res 38:133–143

Güntürkün O (2005a) Avian and mammalian "prefrontal cortices": limited degrees of freedom in the evolution of the neural mechanisms of goal-state maintenance. Brain Res Bull 66:311–316

Güntürkün O (2005b) The avian 'prefrontal cortex' and cognition. Curr Opin Neurobiol 15:686–693

Güntürkün O, Kröner S (1999) A polysensory pathway to the forebrain of the pigeon: the ascending projections of the nucleus dorsolateralis posterior thalami (DLP). Eur J Morphol 37:185–189

Hartmann B, Güntürkün O (1998) Selective deficits in reversal learning after neostriatum caudolaterale lesions in pigeons: possible behavioral equivalencies to the mammalian prefrontal system. Behav Brain Res 96:125–133

Harvey PH, Krebs JR (1990) Comparing brains. Science 249:140–146

Hasselmo ME, Stern CE (2006) Mechanisms underlying working memory for novel information. Trends Cogn Sci 10:487–493

Henley JM, Barnard EA (1990) Autoradiographic distribution of binding sites for the non-NMDA receptor antagonist CNQX in chick brain. Neurosci Lett 116:17–22

Herold C, Diekamp B, Güntürkün O (2008) Stimulation of dopamine D1 receptors in the avian fronto-striatal system adjusts daily cognitive fluctuations. Behav Brain Res 194:223–229

Horn G (1981) Neural mechanisms of learning: an analysis of imprinting in the domestic chick. Proc R Soc Lond B Biol Sci 213:101–137

Horn G, Bradley P, McCabe BJ (1985) Changes in the structure of synapses associated with learning. J Neurosci 5:3161–3168

Hunt GR, Gray RD (2003) Diversification and cumulative evolution in New Caledonian crow tool manufacture. Proc Biol Sci 270:867–874

Jarvis ED, Güntürkün O, Bruce L, Csillag A, Karten H, Kuenzel W, Medina L, Paxinos G, Perkel DJ, Shimizu T, Striedter G, Wild JM, Ball GF, Dugas-Ford J, Durand SE, Hough GE, Husband S, Kubikova L, Lee DW, Mello CV, Powers A, Siang C, Smulders TV, Wada K, White SA, Yamamoto K, Yu J, Reiner A, Butler AB (2005) Avian brains and a new understanding of vertebrate brain evolution. Nat Rev Neurosci 6:151–159

Ji XH, Cao XH, Zhang CL, Feng ZJ, Zhang XH, Ma L, Li BM (2008) Pre- and postsynaptic beta-adrenergic activation enhances excitatory synaptic transmission in layer V/VI pyramidal neurons of the medial prefrontal cortex of rats. Cereb Cortex 18:1506–1520

Kalenscher T, Diekamp B, Güntürkün O (2003) Neural architecture of choice behaviour in a concurrent interval schedule. Eur J Neurosci 18:2627–2637

Kalenscher T, Güntürkün O, Calabrese P, Gehlen W, Kalt T, Diekamp B (2005) Neural correlates of a default response in a delayed go/no-go task. J Exp Anal Behav 84:521–535

Karakuyu D, Herold C, Güntürkün O, Diekamp B (2007) Differential increase of extracellular dopamine and serotonin in the 'prefrontal cortex' and striatum of pigeons during working memory. Eur J Neurosci 26:2293–2302

Karten HJ (1969) The ascending auditory pathway in the pigeon (*Columba livia*). II. Telencephalic projections of the nucleus ovoidalis thalami. Brain Res 11:134–53

Karten H, Hodos W (1967) A stereotaxic atlas of the brain of the pigeon (*Columba livia*). The Johns Hopkins University Press, Baltimore

Kenward B, Weir AA, Rutz C, Kacelnik A (2005) Behavioural ecology: tool manufacture by naive juvenile crows. Nature 433:121

Kirsch JA, Güntürkün O, Rose J (2008) Insight without cortex: lessons from the avian brain. Conscious Cogn 17:475–483

Kohler EC, Riters LV, Chaves L, Bingman VP (1996) The muscarinic acetylcholine antagonist scopolamine impairs short-distance homing pigeon navigation. Physiol Behav 60:1057–1061

Korzeniewska E, Güntürkün O (1990) Sensory properties and afferents of the N. dorsolateralis posterior thalami of the pigeon. J Comp Neurol 292:457–479

Kröner S, Güntürkün O (1999) Afferent and efferent connections of the caudolateral neostriatum in the pigeon (*Columba livia*): a retro- and anterograde pathway tracing study. J Comp Neurol 407:228–260

Leutgeb S, Husband S, Riters LV, Shimizu T, Bingman VP (1996) Telencephalic afferents to the caudolateral neostriatum of the pigeon. Brain Res 730:173–181

Levy R, Goldman-Rakic PS (1999) Association of storage and processing functions in the dorsolateral prefrontal cortex of the nonhuman primate. J Neurosci 19:5149–5158

Lidow MS, Gallager DW, Rakic P, Goldman-Rakic PS (1989) Regional differences in the distribution of muscarinic cholinergic receptors in the macaque cerebral cortex. J Comp Neurol 289:247–259

Lissek S, Güntürkün O (2005) Out of context: NMDA receptor antagonism in the avian 'prefrontal cortex' impairs context processing in a conditional discrimination task. Behav Neurosci 119:797–805

Martinez de la Torre M, Mitsacos A, Kouvelas ED, Zavitsanou K, Balthazart J (1998) Pharmacological characterization, anatomical distribution and sex differences of the non-NMDA excitatory amino acid receptors in the quail brain as identified by CNQX binding. J Chem Neuroanat 15:187–200

McNab F, Klingberg T (2008) Prefrontal cortex and basal ganglia control access to working memory. Nat Neurosci 11:103–107

Medina L, Reiner A (2000) Do birds possess homologues of mammalian primary visual, somatosensory and motor cortices? Trends Neurosci 23:1–12

Mehlhorn J, Hunt GR, Gray RD, Rehkämper G, Güntürkün O (2010) Tool-making new caledonian crows have large associative brain areas. Brain Behav Evol 75:63–70

Merker B (1983) Silver staining of cell bodies by means of physical development. J Neurosci Methods 9:235–241

Metzger M, Jiang S, Braun K (1998) Organization of the dorsocaudal neostriatal complex: a retrograde and anterograde tracing study in the domestic chick with special emphasis on pathways relevant to imprinting. J Comp Neurol 395:380–404

Metzger M, Jiang S, Braun K (2002) A quantitative immuno-electron microscopic study of dopamine terminals in forebrain regions of the domestic chick involved in filial imprinting. Neuroscience 111:611–623

Mitsacos A, Dermon CR, Stassi K, Kouvelas ED (1990) Localization of L-glutamate binding sites in chick brain by quantitative autoradiography. Brain Res 513:348–352

Mogensen J, Divac I (1982) The prefrontal 'cortex' in the pigeon. Behavioral evidence. Brain Behav Evol 21:60–66

Mrzljak L, Pappy M, Leranth C, Goldman-Rakic PS (1995) Cholinergic synaptic circuitry in the macaque prefrontal cortex. J Comp Neurol 357:603–617

Naito E, Scheperjans F, Eickhoff SB, Amunts K, Roland P, Zilles K, Ehrsson HH (2008) Cytoarchitectonic areas in human superior parietal lobule are functionally implicated by an illusion of bimanual interaction with an external object. J Neurophysiol 99:695–703

Palomero-Gallagher N, Zilles K (2004) Isocortex. In: Paxinos G (ed) The rat nervous system, 3rd edn edn. Acadamic Press, San Diego, pp 729–757

Palomero-Gallagher N, Mohlberg H, Zilles K, Vogt B (2008) Cytology and receptor architecture of human anterior cingulate cortex. J Comp Neurol 508:906–926

Palomero-Gallagher N, Vogt B, Mayberg HS, Schleicher A, Zilles K (2009) Receptor architecture of human cingulate cortex: insights into the four-region neurobiological model. Hum Brain Mapp 30:2336–2355

Pinaud R, Mello CV (2007) GABA immunoreactivity in auditory and song control brain areas of zebra finches. J Chem Neuroanat 34:1–21

Pollok B, Prior H, Güntürkün O (2000) Development of object permancence in the food storing magpie (Pica pica). J Comp Psychol 114:148–157

Prior H, Schwarz A, Güntürkün O (2008) Mirror-induced behavior in the magpie (*Pica pica*): evidence of self-recognition. PLoS Biol 6:e202

Puelles L, Kuwana E, Puelles E, Bulfone A, Shimamura K, Keleher J, Smiga S, Rubenstein JL (2000) Pallial and subpallial derivatives in the embryonic chick and mouse telencephalon, traced by the expression of the genes Dlx-2, Emx-1, Nkx-2.1, Pax-6, and Tbr-1. J Comp Neurol 424:409–438

Rehkämper G, Zilles K (1991) Parallel evolution in mammalian and avian brains: comparative cytoarchitectonic and cytochemical analysis. Cell Tissue Res 263:3–28

Reiner A, Perkel DJ, Bruce LL, Butler AB, Csillag A, Kuenzel W, Medina L, Paxinos G, Shimizu T, Striedter G, Wild M, Ball GF, Durand S, Güntürkün O, Lee DW, Mello CV, Powers A, White SA, Hough G, Kubikova L, Smulders TV, Wada K, Dugas-Ford J, Husband S, Yamamoto K, Yu J, Siang C, Jarvis ED (2004) Revised nomenclature for avian telencephalon and some related brainstem nuclei. J Comp Neurol 473:377–414

Richfield EK, Young AB, Penney JB (1989) Comparative distributions of dopamine D-1 and D-2 receptors in the cerebral cortex of rats, cats, and monkeys. J Comp Neurol 286:409–426

Riters LV, Bingman VP (1999) The effects of lesions to the caudolateral neostriatum on sun compass based spatial learning in homing pigeons. Behav Brain Res 98:1–15

Riters LV, Erichsen JT, Krebs JR, Bingman VP (1999) Neurochemical evidence for at least two regional subdivisions within the homing pigeon (*Columba livia*) caudolateral neostriatum. J Comp Neurol 412:469–487

Robbins TW, Arnsten AF (2009) The neuropsychopharmacology of fronto-executive function: monoaminergic modulation. Annu Rev Neurosci 32:267–287

Rose SP (2000) God's organism? The chick as a model system for memory studies. Learn Mem 7:1–17

Rose J, Colombo M (2005) Neural correlates of executive control in the avian brain. PLoS Biol 3:e190

Rose J, Schiffer AM, Dittrich L, Güntürkün O (2010) The role of dopamine in maintenance and distractability of attention in the "prefrontal cortex" of pigeons. Neuroscience 167:232–237

Sakaue M, Somboonthum P, Nishihara B, Koyama Y, Hashimoto H, Baba A, Matsuda T (2000) Postsynaptic 5-hydroxytryptamine (1A) receptor activation increases in vivo dopamine release in rat prefrontal cortex. Br J Pharmacol 129:1028–1034

Salvatierra NA, Torre RB, Arce A (1997) Learning and novelty induced increase of central benzodiazepine receptors from chick forebrain, in a food discrimination task. Brain Res 757:79–84

Santi A, Weise L (1995) The effects of scopolamine on memory for time in rats and pigeons. Pharmacol Biochem Behav 51:271–277

Sarter M, Bruno JP (2000) Cortical cholinergic inputs mediating arousal, attentional processing and dreaming: differential afferent regulation of the basal forebrain by telencephalic and brainstem afferents. Neuroscience 95:933–952

Sarter M, Parikh V, Howe WM (2009) nAChR agonist-induced cognition enhancement: integration of cognitive and neuronal mechanisms. Biochem Pharmacol 78:658–667

Schleicher A, Palomero-Gallagher N, Morosan P, Eickhoff SB, Kowalski T, de Vos K, Amunts K, Zilles K (2005) Quantitative architectural analysis: a new approach to cortical mapping. Anat Embryol (Berl) 210:373–386

Schnabel R, Metzger M, Jiang S, Hemmings HC Jr, Greengard P, Braun K (1997) Localization of dopamine D1 receptors and dopaminoceptive neurons in the chick forebrain. J Comp Neurol 388:146–168

Seed AM, Tebbich S, Emery NJ, Clayton NS (2006) Investigating physical cognition in rooks, *Corvus frugilegus*. Curr Biol 16:697–701

Sorenson EM, Chiappinelli VA (1992) Localization of 3H-nicotine, 125I-kappa-bungarotoxin, and 125I-alpha-bungarotoxin binding to nicotinic sites in the chicken forebrain and midbrain. J Comp Neurol 323:1–12

Stewart MG, Bourne RC, Chmielowska J, Kalman M, Csillag A, Stanford D (1988) Quantitative autoradiographic analysis of the distribution of [3H]muscimol binding to GABA receptors in chick brain. Brain Res 456:387–391

Stewart MG, Cristol D, Philips R, Steele RJ, Stamatakis A, Harrison E, Clayton N (1999) A quantitative autoradiographic comparison of binding to glutamate receptor sub-types in hippocampus and forebrain regions of a food-storing and a non-food-storing bird. Behav Brain Res 98:89–94

Taylor AH, Hunt GR, Medina FS, Gray RD (2009) Do New Caledonian crows solve physical problems through causal reasoning? Proc Biol Sci 276:247–254

Uylings HBM, Sanz-Arigita E, de Vos K, Smeets WJAJ, Pool CW, Amunts K, Rajkowska G, Zilles K (2000) The importance of a human 3D database and atlas for studies of prefrontal and thalamic functions. Progr Brain Res 126:357–368

Uylings HB, Groenewegen HJ, Kolb B (2003) Do rats have a prefrontal cortex? Behav Brain Res 146:3–17

Van De Werd HJ, Rajkowska G, Evers P, Uylings HB (2010) Cytoarchitectonic and chemoarchitectonic characterization of the prefrontal cortical areas in the mouse. Brain Struct Funct 214:339–353

Van Eden CG, Lamme VA, Uylings HB (1992) Heterotopic cortical afferents to the medial prefrontal cortex in the rat. A combined retrograde and anterograde tracer study. Eur J Neurosci 4:77–97

Veenman CL, Albin RL, Richfield EK, Reiner A (1994) Distributions of GABAA, GABAB, and benzodiazepine receptors in the forebrain and midbrain of pigeons. J Comp Neurol 344:161–189

Veenman CL, Wild JM, Reiner A (1995) Organization of the avian "corticostriatal" projection system: a retrograde and anterograde pathway tracing study in pigeons. J Comp Neurol 354:87–126

Vogt BA, Pandya DN (1987) Cingulate cortex of the rhesus monkey: II. Cortical afferents. J Comp Neurol 262:271–289

Waeber C, Dietl MM, Hoyer D, Palacios JM (1989) 5.HT1 receptors in the vertebrate brain. Regional distribution examined by autoradiography. Naunyn Schmiedebergs Arch Pharmacol 340:486–494

Waldmann C, Güntürkün O (1993) The dopaminergic innervation of the pigeon caudolateral forebrain: immunocytochemical evidence for a 'prefrontal cortex' in birds? Brain Res 600:225–234

Wang M, Ramos BP, Paspalas CD, Shu Y, Simen A, Duque A, Vijayraghavan S, Brennan A, Dudley A, Nou E, Mazer JA, McCormick DA, Arnsten AF (2007) Alpha2A-adrenoceptors strengthen working memory networks by inhibiting cAMP-HCN channel signaling in prefrontal cortex. Cell 129:397–410

Williams GV, Castner SA (2006) Under the curve: critical issues for elucidating D1 receptor function in working memory. Neuroscience 139:263–276

Wynne B, Güntürkün O (1995) Dopaminergic innervation of the telencephalon of the pigeon (*Columba livia*): a study with antibodies against tyrosine hydroxylase and dopamine. J Comp Neurol 357:446–464

Yamamoto K, Reiner A (2005) Distribution of the limbic-system associated membran protein (LAMP) in pigeon forebrain and midbrain. J Comp Neurol 486:221–242

Yamasaki M, Matsui M, Watanabe M (2010) Preferential localization of muscarinic M1 receptor on dendritic shaft and spine of cortical pyramidal cells and its anatomical evidence for volume transmission. J Neurosci 30:4408–4418

Zahrt J, Taylor JR, Mathew RG, Arnsten AF (1997) Supranormal stimulation of D1 dopamine receptors in the rodent prefrontal cortex impairs spatial working memory performance. J Neurosci 17:8528–8535

Zhang W, Yamada M, Gomeza J, Basile AS, Wess J (2002) Multiple muscarinic acetylcholine receptor subtypes modulate striatal dopamine release, as studied with M1–M5 muscarinic receptor knock-out mice. J Neurosci 22:6347–6352

Zilles K (1985) The cortex of the rat, a stereotaxic atlas. Springer Verlag, Berlin

Zilles K, Amunts K (2010) Centenary of Brodmann's map—conception and fate. Nat Rev Neurosci 11:139–145

Zilles K, Schleicher A, Palomero-Gallagher N, Amunts K (2002a) Quantitative analysis of cyto- and receptor architecture of the human brain. In: Mazziotta JC, Toga A (eds) Brain mapping: the methods. Elsevier, Amsterdam, pp 573–602

Zilles K, Palomero-Gallagher N, Grefkes C, Scheperjans F, Boy C, Amunts K, Schleicher A (2002b) Architectonics of the human cerebral cortex and transmitter receptor fingerprints: reconciling functional neuroanatomy and neurochemistry. Eur Neuropsychopharmacol 12:587–599